First-principles phase diagram of the Ce-Th system

A. Landa and P. Söderlind
Physics and Advances Technologies, Lawrence Livermore National Laboratory, University of California, P.O. Box 808, Livermore, California 94550, USA

A. Ruban
Applied Materials Physics, Department of Materials Science and Engineering, Royal Institute of Technology, SE-10044, Stockholm, Sweden

L. Vitos
Applied Materials Physics, Department of Materials Science and Engineering, Royal Institute of Technology, SE-10044, Stockholm, Sweden
Research Institute for Solid State Physics and Optics, H-1525 Budapest, P.O. Box 49, Hungary

L. Pourovskii
Electronic Structure of Materials, Department of Theoretical Physics, University of Nijmegen, 6525ED, Nijmegen, The Netherlands
(Received 18 May 2004; revised manuscript received 17 August 2004; published 28 December 2004)

Ab initio total energy calculations based on the exact muffin-tin orbitals (EMTO) theory are used to determine the high pressure and low-temperature phase diagram of Ce and Th metals as well as the $Ce_{43}Th_{57}$ disordered alloy. The compositional disorder for the alloy is treated in the framework of the coherent potential approximation. The equation of state for Ce, Th, and $Ce_{43}Th_{57}$ has been calculated up to 1 Mbar in good comparison with experimental data: upon compression the Ce-Th system undergoes crystallographic phase transformation from a fcc to a body-centered-tetragonal structure and the transition pressure increases with Th content in the alloy.

DOI: 10.1103/PhysRevB.70.224210 PACS number(s): 71.10.−w, 71.28.+d

I. INTRODUCTION

Actinide physics has seen a remarkable focus the last decade or so due to the combination of experimental diamond-anvil-cell techniques and the development of fast computers and more advanced theory. All *f*-electron systems are expected to have multiphase phase diagrams due to the sensitivity of the *f*-electron band to external influences such as pressure and temperature. For instance, compression of an *f*-electron metal generally causes the occupation of the *f* states to change due to a shift of these bands relative to others. This can in some cases, as in the Ce-Th system,[1,2] cause the crystal to adopt a lower symmetry structure at elevated pressures. Under compression, the *f*-electron dominance increases in these systems and drives the phase transition. The reason for this has been discussed[3] in terms of a Peierls or Jahn-Teller distortion that favors low symmetry over high symmetry crystal structures. On the other hand, all bands broaden under compression and the distortion of the lattice becomes less important, while electrostatic forces tend to move atoms to higher symmetry positions, ultimately leading to closer packed structures with higher symmetry. This interplay between competing effects and their pressure dependence often results in interesting multiphase phase diagrams. This is the case for Ce, Th, and Ce-Th alloys.

This Brief Report is devoted to the study of phase stabilities of Ce, Th, and the Ce-Th system as a function of compression. Cerium metal has a very interesting phase diagram with two isostructural, face-centered-cubic (fcc) phases, namely γ-Ce and α-Ce. The latter is considerably denser than the former and there is a substantial volume collapse associated with the $\gamma \rightarrow \alpha$ transition that occurs at a moderate pressure close to 10 kbar. The nature of this transition is currently not fully understood, but it can be described[4] as a Mott transition of the *f* electron from a localized (γ-Ce) to an itinerant (α-Ce) state. Below 100 kbar, there is also a phase transition to a lower symmetry phase, which is believed to be either orthorhombic or body-centered monoclinic.[5] Above 120 kbar, however, Ce is stabilized in a body-centered-tetragonal (bct) structure and remains in this phase up to the highest measured pressure. Thorium metal is similar to cerium in this regard, but has a simpler phase diagram. Only one phase transition has been seen at low temperatures: fcc $\rightarrow$ bct at about 600 kbar. At Mbar pressures, both these metals remain in a bct crystal[6,7] with a c/a axial ratio close to 1.65. Also the Ce-Th system shows a similar behavior.[1] Theoretically, the Ce-Th alloys are rather well described within the density-functional theory (DFT),[2,8] although a proper treatment of the disordered Ce-Th alloys has not yet been presented. In fact, it was argued[2] that the disorder in the realistic Ce-Th alloys could not be well modeled by an ordered compound. The theoretical low pressure behavior of Ce_cTh_{1-c} was therefore erroneous[2] for $c=0.43$. In the present paper we revisit this problem by applying a more sophisticated theory of random alloys based on the coherent potential approximation (CPA).

The paper is organized as follows. Our computational approach is discussed in Sect. II, followed by results and discussioning Sect. III. We present our conclusions in Sect. IV.

II. COMPUTATIONAL DETAILS

The calculations we have referred to as exact muffin-tin orbitals (EMTO) are performed using both scalar-relativistic (SR) and full-relativistic (FR), Green's function technique based on an improved screened Korringa-Kohn-Rostoker (KKR) method, where the one-electron potential is represented by optimized overlapping muffin-tin (OOMT) potential spheres.[9–13] Inside the potential spheres the potential is spherically symmetric and it is constant between the spheres. The radii of the potential spheres, the spherical potentials inside the spheres, and the constant value from the interstitial are determined by minimizing (i) the deviation between the exact and overlapping potentials, and (ii) the errors coming from the overlap between spheres. Thus, the OOMT potential ensures a more accurate description of the full potential compared to the conventional muffin-tin or nonoverlapping approach.

Within the EMTO formalism, the one-electron states are calculated *exactly* for the OOMT potentials. As an output of the EMTO calculations, one can determine the self-consistent Green's function of the system and the complete, nonspherically symmetric charge density. Finally, the total energy is calculated using the full charge density technique.[12,14] For the exchange/correlation approximation, we use the generalized gradient approximation (GGA),[15] which has proven to be better for *f*-electron metals.[16] Within the FR-EMTO formalism, spin-orbit coupling is taken into account exactly by solving the four-component Dirac equation.[17] For the total energy of random substitutional alloys, the EMTO method has been recently combined with the CPA.[13,18]

The calculations are performed for a basis set including valence *spdf* orbitals and the semicore 6*p* state whereas the core states were recalculated at each iteration. Integration over the irreducible wedge of the Brillouin zone (IBZ) is performed using the special *k*-point method[19] with 916 and 5525 *k*-points (per IBZ) for fcc and bct lattices, respectively. The Green's function has been calculated for 40 complex energy points distributed exponentially on a semi-circle enclosing the occupied states. The equilibrium density is obtained from a Murnaghan fit[20] fit to about 15 total energies calculated as a function of the lattice constant. The c/a axial ratio was optimaized for the selected volume (pressure) by calculation the so-called Bain transformation path (total energy versus c/a axial ratio of a bct system).[21]

III. RESULTS AND DISCUSSION

Before entering the details of the crystal structure of Ce and Th under compression, we compare our calculated equation of state (EOS) with the experimental data for these two metals. In Fig. 1 we show the theoretical and measured equations of state for cerium metal. The agreement between theory and experiment[6] is very good, especially in the region of pressures less than 300 kbar. Notice that the results of the FR and SR calculations are almost identical. Calculated (SR) equilibrium volume and bulk modulus at ambient pressure are $V_0=27.7$ Å^3 and $B_0=380$ kbar, respectively, and compares well with the low-temperature data[22] ($V_0=28.0$ Å^3 and $B_0=290$ kbar). FR calculations result in a slighter smaller equilibrium volume (27.4 Å^3). Notice also that both EMTO-SR and EMTO-FR calculations give better equilibrium properties of cerium metal at ambient pressure then the previous full-potential linearized muffin-tin orbital (FPLMTO) study[8] ($V_0=26.1$ Å^3 and $B_0=490$ kbar), however, the FPLMTO method gives better EOS at elevated pressures.

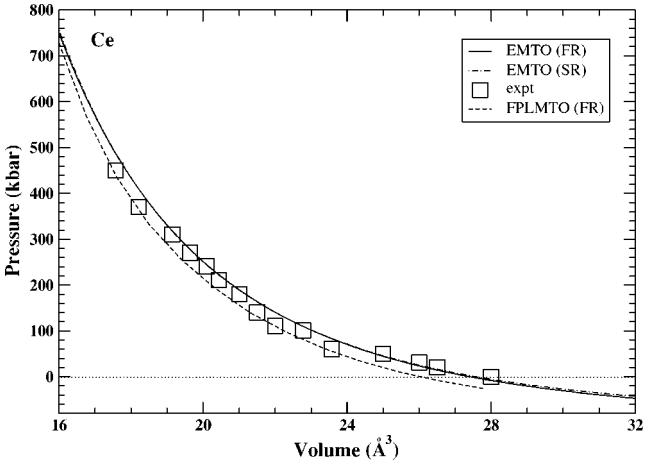

FIG. 1. Equation of state for Ce. Experimental results (Ref. 6) are marked with open squares and theory is given by solid and dot-dashed lines. The results of earlier FPLMTO calculations (Ref. 8) are shown by the dashed line.

Also for thorium metal, the EOS is in a good agreement with experiment[23] (see Fig. 2). Calculated (SR) equilibrium volume and bulk modulus at ambient pressure are $V_0=33.3$ Å^3 and $B_0=580$ kbar, respectively, and close to the experimental data[23] ($V_0=32.9$ Å^3 and $B_0=580$ kbar). FR calculations result in a slighter smaller equilibrium volume (33.1 Å^3). As in the case for cerium metal, the EMTO ambient pressure results compare better with experiment than those of the FPLMTO study[8] ($V_0=29.6$ Å^3 and $B_0=630$ kbar), which seem better at elevated pressures

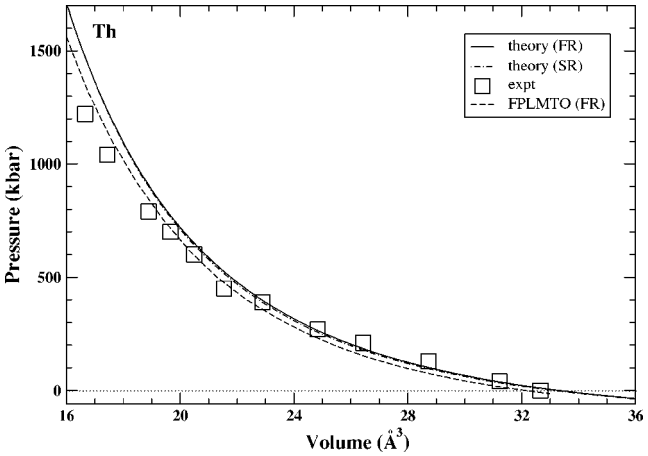

FIG. 2. Equation of state for Th. Experimental results (Ref. 23) are marked with open squares and theory is given by solid and dot-dashed lines. The results of earlier FPLMTO calculations (Ref. 8) are shown by the dashed line.

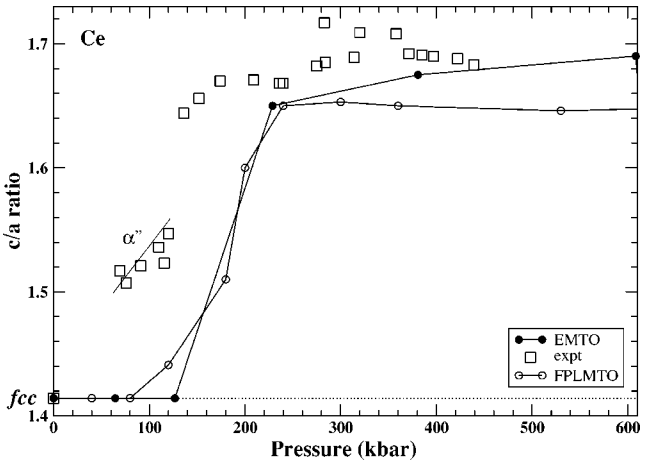

FIG. 3. The c/a axial ratio for the bct structure as a function of pressure for Ce. Experimental data (Ref. 6) are marked with open squares while theoretical results are given by a solid line and filled circles. The results of FPLMTO calculations (Ref. 8) are shown by a solid line and open circles.

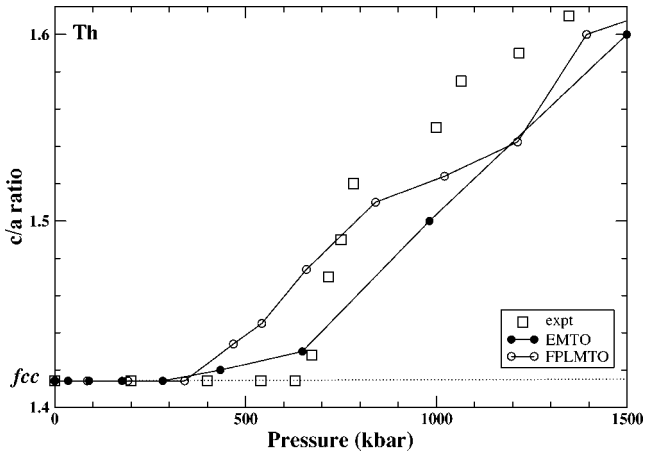

FIG. 4. The c/a axial ratio for the bct structure as a function of pressure for Th. Experimental data (Ref. 7) are marked with open squares and theoretical results are given by a solid line and filled circles. The results of FPLMTO calculations (Ref. 8) are shown by a solid line and open circles.

(more than 700 kbar). Considering the fact that the spin-orbit coupling has a negligible effect on the calculated EOS, the following calculations exclude this interaction.

Next we study the crystal-structure behavior for cerium metal, and in Fig. 3 we plot the calculated c/a axial ratio for bct Ce together with experimental data.[6] At pressures beyond about 120 kbar, cerium adopts a bct structure with a c/a ratio close to 1.65. Quantitatively, this behavior is well reproduced by our calculations. Also, there is known to be an intermediate lower symmetry phase[6] in Ce (below 100 kbar), which is limited to a small pressure range and not considered in the present calculations (it has been investigated theoretically before).[24] Present results are also in an excellent agreement with the results of the previous FPLMTO calculations[8] shown in Fig. 3.

A similar behavior is found for thorium metal (see Fig. 4). Experimentally,[7] Th is stable in its ambient pressure phase (fcc) up to 630 kbar. At higher compression, Th transforms *continuously* into the bct phase. The transition pressure is considerably higher in Th than in Ce. The fact that the fcc→bct transition occurs at a higher pressure in Th than in Ce has been discussed before[2,8] and will be addressed below. As in the case of cerium metal, present results agree well with those of previous FPLMTO calculations[8] also shown in Fig. 4.

As we have established that Ce and Th metal can be very well described by DFT methods, we next consider the $Ce_{43}Th_{57}$ disordered fcc alloy. In Fig. 5 we show theoretical EOS for the $Ce_{43}Th_{57}$ disordered fcc alloy. Notice that the EOS curve for $Ce_{43}Th_{57}$ is located between those for elemental Th and Ce, which are also shown. Calculated equilibrium atomic volume and bulk modulus for $Ce_{43}Th_{57}$ are 31.4 Å^3 and 460 kbar, respectively, which are in reasonable agreement with experimental data of 32.9 Å^3 and 281 kbar.[1] In order to understand this difference, one should notice that the Ce-Th system is composed by γ-Ce and α-Th, and there is a significant negative deviation from the Vegard's law in this system within the whole concentration interval[25] due to delocalization of $4f$-Ce electrons under the local pressure imposed on γ-Ce atoms by smaller α-Th atoms (the experimental atomic volume of γ-Ce and α-Th is 34.37 Å^3 and 32.89 Å^3, respectively[23,26]). According to our calculations, the $Ce_{43}Th_{57}$ disordered fcc alloy, created by α-Ce and α-Th, obeys the Vegard's law reflecting the itinerant nature of $4f$-Ce and $5f$-Th electrons within the current DFT formalism.

Before discussing the fcc→bct transition in the $Ce_{43}Th_{57}$ alloy, we plot f-band occupation number of Ce, Th, and this alloy as a function of pressure (Fig. 6). At pressure ~1.5 Mbar the f-band population for thorium metal reaches almost the same value (~1.6) as for cerium metal at much lower pressure (~0.6 Mbar). This is no surprise, because the f-band population in Th at ambient pressure is approximately half that of Ce. This explains why the fcc→bct transition in Th occurs at a much higher pressure then in Ce. According to our calculations for $Ce_{43}Th_{57}$, the f-band occupation reaches the same value (~1.6) at pressure of about 1.1 Mbar.

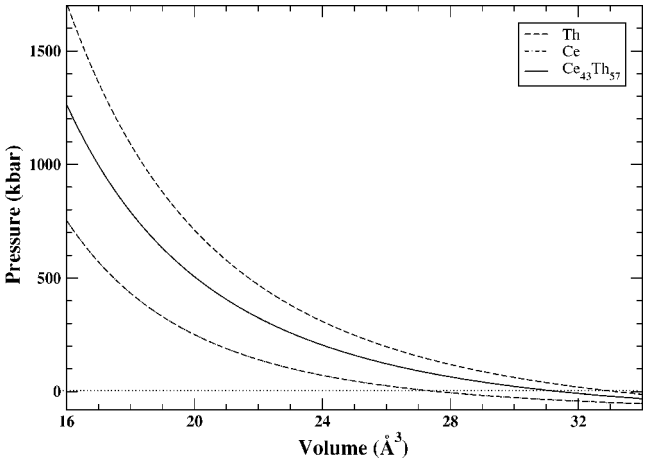

FIG. 5. Equation of state for the $Ce_{43}Th_{57}$ disordered alloy. EOS for Ce and Th are also shown.

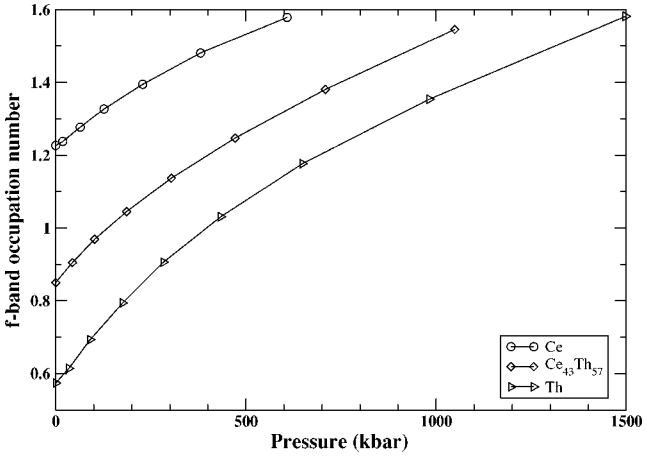

FIG. 6. Calculated f-band occupation of Ce, Th, and the $Ce_{43}Th_{57}$ disordered alloy as a function of pressure.

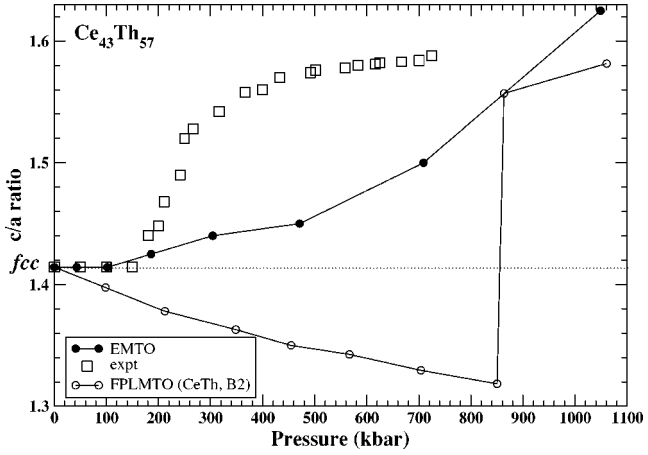

FIG. 7. The c/a axial ratio for the bct structure as a function of pressure for the $Ce_{43}Th_{57}$ disordered alloy. Experimental data (Ref. 1) are marked with open squares while EMTO theoretical results are given by a solid line and filled circles. Also, the results of FPLMTO (Ref. 2) calculations for CeTh-ordered (B2) compound are given by a solid line and open circles.

Finally, Fig. 7 shows the calculated and measured c/a axial ratio as a function of pressure for the $Ce_{43}Th_{57}$ disordered alloy. The structural behavior of this alloy was previously modeled by an ordered (B2) CeTh compound.[2] These earlier calculations predicted unrealistic low-pressure behavior for this system, where the axial c/a ratio first decreased with pressure and suddenly jumped to a high value closer to the measure value at a higher compression. It was speculated[2] that the discrepancy with experiment was due to the failure of modeling the disordered alloy with an ordered compound. Here we can address this question explicitly because the EMTO-CPA formalism allows us to treat the alloy more realistically. The EMTO-CPA calculations confirm that the fcc$\rightarrow$bct phase transition begins between 100–200 kbar, which is close to the corresponding transition in Ce metal (120 kbar), but considerably lower than for Th (630 kbar). Our calculations thus reproduce the experimental observation[1] that the fcc$\rightarrow$bct transition pressure is a strongly nonlinear function of Th concentration in the Ce-Th system. Test calculations (not shown) for the ordered (B2) compound reproduce the incorrect low-pressure behavior found earlier[2] for $Ce_{43}Th_{57}$ whereas the disordered $Ce_{50}Th_{50}$ does not. This indeed validates our assumption[2] that the disorder needs to be properly accounted for to accurately describe $Ce_{43}Th_{57}$. To further improve our description of the phase transition in the $Ce_{43}Th_{57}$ alloy, the ability to reproduce the $\alpha\rightarrow\gamma$ transition in cerium metal needs to be included in the model, because this transition will influence the f-band population in the system.

IV. CONCLUSION

We have presented accurate electronic-structure calculations for the Ce-Th system. Generally, the theory reproduces experimental data very well. The structural pressure dependence is well understood and driven by the increased presence of f electrons under pressure. Ce, Th, and the $Ce_{43}Th_{57}$ disordered alloy behave rather similarly, although Ce has intermediate phases in the phase diagram at about 100 kbar that do not exist in Th and the $Ce_{43}Th_{57}$ alloy. Consequently, the fcc$\rightarrow$bct transition is of the first order in Ce but not in Th and the $Ce_{43}Th_{57}$ alloy. For this alloy a CPA treatment is necessary to reproduce, at least qualitatively, the correct structural behavior.

ACKNOWLEDGMENT

This work was performed under the auspices of the U.S. Department of Energy by the University of California Lawrence Livermore National Laboratory under Contract No. W-7405-Eng-48. A.R. and L.V. are grateful to the Swedish Research Council, the Swedish Foundation for Strategic Research, and the Royal Swedish Academy of Sciences. L.V. also acknowledges the Research Project OTKA T046773 of the Hungarian Scientific Research Fund.

[1] G. Gu, Y. K. Vohra, U. Benedict, and J. C. Spirlet, Phys. Rev. B **50**, 2751 (1994); G. Gu, Y. K. Vohra, J. M. Winand, and J. C. Spirlet, Scr. Metall. Mater. **32**, 2081 (1995).

[2] P. Söderlind and O. Eriksson, Phys. Rev. B **60**, 9372 (1999).

[3] P. Söderlind, O. Eriksson, B. Johansson, J. M. Wills, and A. M. Boring, Nature (London) **374**, 524 (1995).

[4] B. Johansson, I. A. Abrikosov, M. Alden, A. V. Ruban, and H. L. Skriver, Phys. Rev. Lett. **74**, 2335 (1995).

[5] M. I. McMahon and R. J. Nelmes, Phys. Rev. Lett. **78**, 3884 (1998).

[6] J. Staun Olsen, L. Gerward, U. Benedict, and J.-P. Itie, Physica B & C **133**, 129 (1985).

[7] Y. K. Vohra and J. Akella, Phys. Rev. Lett. **67**, 3563 (1991); High Press. Res. **10**, 681 (1992).
[8] P. Söderlind, O. Eriksson, B. Johansson, and J. M. Wills, Phys. Rev. B **52**, 13 169 (1995).
[9] O. K. Andersen, O. Jepsen, and G. Krier, in *Methods of Electronic Structure Calculations*, edited by V. Kumar, O. K. Andersen, and A. Mookerjee (World Scientific, Singapore, 1994), pp. 6–124.
[10] O. K. Andersen, C. Arcangeli, R. W. Tank, T. Saha-Dasgupta, G. Krier, O. Jepsen, and I. Dasgupta, in *Tight-Binding Approach to Computational Materials Science*, edited by P. E. A. Turchi, A. Gonis, and L. Colombo, M. R. S. Symposia Proceedings No. 491 (Materials Research Society, Warrendale, 1998), pp. 3–34.
[11] L. Vitos, H. L. Skriver, B. Johansson, and J. Kollar, Comput. Mater. Sci. **18**, 24 (2000).
[12] L. Vitos, Phys. Rev. B **64**, 014107 (2001).
[13] L. Vitos, in *Recent Research and Development in Physics* (Transworld Research Network Publisher, Trivandrum, 2004), Vol. 5, pp. 103–140.
[14] J. Kollar, L. Vitos, and H. L. Skriver, *Electronic Structure and Physical Properties of Solids: The Uses of the LMTO Method*, Lecture Notes in Physics (Springer, Berlin, 2000), pp. 85–113.
[15] J. P. Perdew, K. Burke, and M. Ernzerhof, Phys. Rev. Lett. **77**, 3865 (1996).
[16] P. Söderlind, O. Eriksson, B. Johansson, and J. M. Wills, Phys. Rev. B **50**, 7291 (1994).
[17] L. Pourovskii, A. Ruban, L. Vitos, E. Ebert, I. Abrikosov, and B. Johansson, Phys. Rev. B (to be published).
[18] L. Vitos, I. A. Abrikosov, and B. Johansson, Phys. Rev. Lett. **87**, 156401 (2001).
[19] D. J. Chadi and M. L. Cohen, Phys. Rev. B **8**, 5747 (1973); S. Froyen, *ibid.* **39**, 3168 (1989).
[20] F. D. Murnaghan, Proc. Natl. Acad. Sci. U.S.A. **30**, 244 (1944).
[21] E. C. Bain, Trans. AIME **70**, 25 (1924).
[22] J. Donohue, *The Structure of Elements* (Wiley, New York, 1974).
[23] Y. K. Vohra and W. B. Holzapfel, High Press. Res. **11**, 223 (1993).
[24] P. Söderlind, Adv. Phys. **47**, 959 (1998).
[25] D. S. Evans and G. V. Raynor, J. Anal. Chem. USSR **5**, 308 (1962).
[26] B. J. Beaudry and P. E. Palmer, J. Less-Common Met. **34**, 225 (1974).